

Chapter 2

Classical and Quantum Ideal Gases

Abstract Bose and Einstein's prediction of Bose–Einstein condensation came out of their theory for how quantum particles in a gas behaved, and was built on the pioneering statistical approach of Boltzmann for classical particles. Here we follow Boltzmann, Bose and Einstein's footsteps, leading to the derivation of Bose–Einstein condensation for an ideal gas and its key properties.

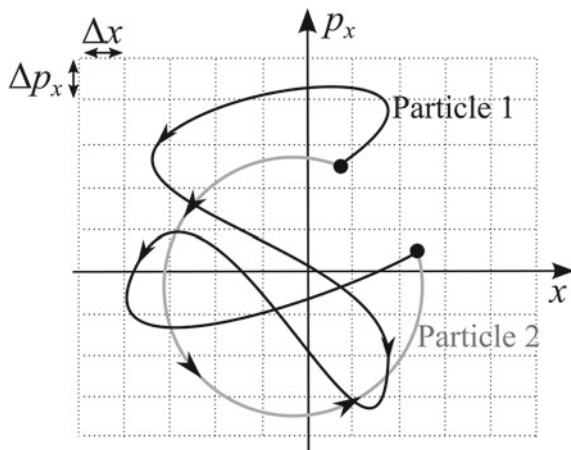
2.1 Introduction

Consider the air in the room around you. We ascribe properties such as temperature and pressure to characterise it, motivated by our human sensitivity to these properties. However, the gas itself has a much finer level of detail, being composed of specks of dust, molecules and atoms, all in random motion. How can we explain the macroscopic, coarse-grained appearance in terms of the fine-scale behaviour? An exact classical approach would proceed by solving Newton's equation of motion for each particle, based on the forces it experiences. For a typical room (volume $\sim 50 \text{ m}^3$, air particle density $\sim 2 \times 10^{25} \text{ m}^{-3}$ at room temperature and pressure) this would require solving around 10^{28} coupled ordinary differential equations, an utterly intractable task. Since the macroscopic properties we experience are *averaged* over many particles, a particle-by-particle description is unnecessarily complex. Instead it is possible to describe the fine-scale behaviour *statistically* through the methodology of statistical mechanics. By specifying rules about how the particles behave and any physical constraints (boundaries, energy, etc.), the most likely macroscopic state of the system can be deduced.

We develop these ideas for an ideal gas of N identical and non-interacting particles, with temperature T and confined to a box of volume \mathcal{V} . The system is isolated, with no energy or particles entering or leaving the system¹ Our aim is to predict the equilibrium state of the gas. After performing this for classical (point-like) particles, we extend it to quantum (blurry) particles. This leads directly to the prediction of Bose–Einstein condensation of an ideal gas. In doing so, we follow the seminal

¹In the formalism of statistical mechanics, this is termed the *microcanonical ensemble*.

Fig. 2.1 Two different classical particle trajectories through 1D phase space (x, p_x) , with the same initial and final states. While classical phase space is a continuum of states, it is convenient to imagine phase space to be discretized into finite-sized cells, here with size Δp_x and Δx



works of Boltzmann, Bose and Einstein. Further information can be found in an introductory statistical physics textbook, e.g., [1] or [2].

2.2 Classical Particles

The state of a classical particle is specified by its position \mathbf{r} and momentum \mathbf{p} . In the 3D Cartesian world, this requires six coordinates (x, y, z, p_x, p_y, p_z) . Picturing the world as an abstract six dimensional *phase space*, the instantaneous state of the particle is a point in this space, which traces out a trajectory as it evolves. Accordingly, an N -particle gas is specified by N points/trajectories in this phase space. The accessible range of phase space is determined by the box (which provides a spatial constraint) and the energy of the gas (which determines the maximum possible momentum). Figure 2.1 (left) illustrates two particle trajectories in 1D phase space (x, p_x) .

Classically, a particle's state (its position and momentum) can be determined to arbitrary precision. As such, classical phase space is continuous and contains an infinite number of accessible states. This also implies that each particle can be independently tracked, that is, that the particles are *distinguishable* from each other.

2.3 Ideal Classical Gas

We develop an understanding of the macroscopic behaviour of the gas from these microscopic rules (particle distinguishability, continuum of accessible states) following the pioneering work of Boltzmann in the late 1800s on the kinetic theory of

gases. Boltzmann's work caused great controversy, as its particle and statistical basis was at odds with the accepted view of matter as being continuous and deterministic. To overcome the practicalities of dealing with the infinity of accessible states, we imagine phase space to be discretized into cells of finite (but otherwise arbitrary) size, as shown in Fig. 2.1, and our N particles to be distributed across them randomly. Let there be M accessible cells, each characterised by its average momentum and position. The number of particles in the i th cell—its *occupancy number*—is denoted as N_i . The number configuration across the whole system is specified by the full set of occupancy numbers $\{N_1, N_2, \dots, N_M\}$. We previously assumed that the total particle number is conserved, that is,

$$N = \sum_{i=1}^{i=M} N_i.$$

Conservation of energy provides a further constraint; for now, however, we ignore energetic considerations.

2.3.1 Macrostates, Microstates and the Most Likely State of the System

The macroscopic, equilibrium state of the gas is revealed by considering the ways in which the particles can be distributed across the cells. In the absence of energetic constraints, each cell is equally likely to be occupied. Consider two classical particles, A and B (the distinguishability of the particles is equivalent to saying we can label them), and three such cells. The nine possible configurations, shown in Fig. 2.2, are termed *microstates*. Six distinct sets of occupancy numbers are possible, $\{N_1, N_2, N_3\} = \{2, 0, 0\}, \{0, 2, 0\}, \{0, 0, 2\}, \{1, 1, 0\}, \{1, 0, 1\}$ and $\{0, 1, 1\}$; these are termed *macrostates*. Each macrostate may be achieved by one or more microstates.

The particles are constantly moving and interacting/colliding with each other in a random manner, such that, after a sufficiently long time, they will have visited all available microstates, a process termed *ergodicity*. It follows that each microstate is

Cell 3	<div></div>	<div></div>	AB	<div></div>	<div></div>	B	A	B	A
Cell 2	<div></div>	AB	<div></div>	B	A	<div></div>	<div></div>	A	B
Cell 1	AB	<div></div>	<div></div>	A	B	A	B	<div></div>	<div></div>

Fig. 2.2 Possible configurations of two classical particles, A and B, across three equally-accessible cells. If we treat the energies of cells 1–3 as 0, 1 and 2, respectively, and require that the total system energy is 1 (in arbitrary units), then only the shaded configurations are possible

equally likely (the assumption of “equal *a priori* probabilities”). Thus the most probable macrostate of the system is the one with the most microstates. In our example, the macrostates $\{1, 1, 0\}$, $\{1, 0, 1\}$ and $\{0, 1, 1\}$ are most probable (having 2 microstates each). In a physical gas, each macrostate corresponds to a particular macroscopic appearance, e.g. a certain temperature, pressure, etc. Hence, these abstract probabilistic notions become linked to the most likely macroscopic appearances of the gas.

For a more general macrostate $\{N_1, N_2, N_3, \dots, N_I\}$, the number of microstates is,

$$W = \frac{N!}{\prod_i N_i!}. \quad (2.1)$$

Invoking the principle of equal *a priori* probabilities, the probability of being in the j th macrostate is,

$$\text{Pr}(j) = \frac{W_j}{\sum_j W_j}. \quad (2.2)$$

W_j , and hence $\text{Pr}(j)$, is maximised for the most even distribution of particles across the cells. This is true when each cell is equally accessible; as we discuss next, energy considerations modify the most preferred distribution across cells.

2.3.2 The Boltzmann Distribution

In the ideal-gas-in-a-box, each particle carries only *kinetic energy* $p^2/2m = (p_x^2 + p_y^2 + p_z^2)/2m$. Having discretizing phase space, particle energy also becomes

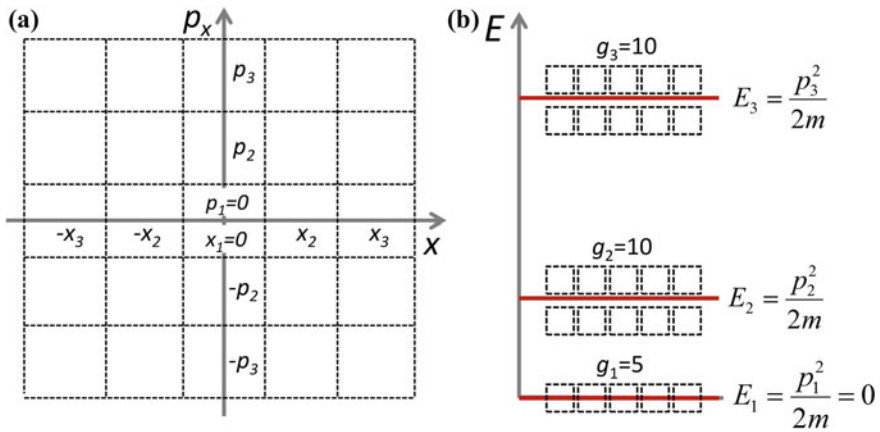


Fig. 2.3 For the phase space (x, p_x) shown in (a), the discretization of phase space, coupled with the energy-momentum relation $E = p^2/2m$, leads to the formation of (b) energy levels. The degeneracy g of the levels is shown

discretized, forming the notion of energy levels (familiar from quantum mechanics). This is illustrated in Fig. 2.3 for (x, p_x) phase space. Three energy levels, $E_1 = 0$, $E_2 = p_1^2/2m$ and $E_3 = p_2^2/2m$, are formed from the five momentum values ($p = 0, \pm p_1, \pm p_2$). In two- and three-spatial dimensions, cells of energy E_i fall on circles and spherical surfaces which satisfy $p_x^2 + p_y^2 = 2mE_i$ and $p_x^2 + p_y^2 + p_z^2 = 2mE_i$, respectively. The lowest energy state E_1 is the *ground state*; the higher energy states are *excited states*.

The total energy of the gas U is,

$$U = \sum_i N_i E_i,$$

where E_i is the energy of cell i . Taking U to be conserved has important consequences for the microstates and macrostates. For example, imposing some arbitrary energy values in Fig. 2.2 restricts the allowed configurations. Particle occupation at high energy is suppressed, skewing the distribution towards low energy.

For a system at thermal equilibrium with a large number of particles, one macrostate (or a very narrow range of macrostates) will be greatly favoured. The preferred macrostate can be analytically predicted by maximising the number of microstates W with respect to the set of occupancy numbers $\{N_1, N_2, N_3, \dots, N_I\}$; details can be found in, e.g. [1, 2]. The result is,

$$N_i = f_B(E_i), \quad (2.3)$$

where $f_B(E)$ is the famous Boltzmann distribution,

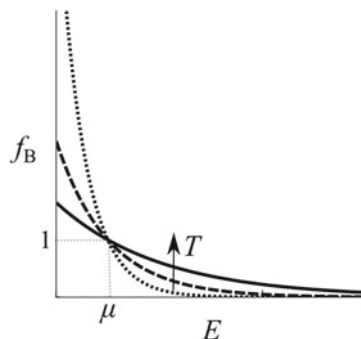
$$f_B(E) = \frac{1}{e^{(E-\mu)/k_B T}}. \quad (2.4)$$

The Boltzmann distribution tells us the most probable spread of particle occupancy across states in an ideal gas, as a function of energy. This is associated with the thermodynamic equilibrium state. Here k_B is Boltzmann's constant ($1.38 \times 10^{-23} \text{ m}^2 \text{ kg s}^{-2} \text{ K}^{-1}$) and T is temperature (in Kelvin degrees, K). On average, each particle carries kinetic energy $\frac{3}{2}k_B T$ ($\frac{1}{2}k_B T$ in each direction of motion); this property is referred to as the *equipartition theorem*.

The Boltzmann distribution function f_B is normalized to the number of particles, N , as accommodated by the chemical potential μ . Writing $A = e^{\mu/k_B T}$ gives $f_B = A/e^{E/k_B T}$, evidencing that A , and thereby μ , controls the amplitude of the distribution function.

The Boltzmann distribution function $f_B(E)$ is plotted in Fig. 2.4. Low energy states (cells) are highly occupied, with diminishing occupancy of higher energy states. As the temperature and hence the thermal energy increases, the distribution broadens as particles can access, on average, higher energy states. Remember, however, that this is the most *probable* distribution. Boltzmann's theory allows for the possibility, for example, that the whole gas of molecules of air in a room concentrates into a

Fig. 2.4 The Boltzmann distribution function $f_B(E)$ for 3 different temperatures (the direction of increasing temperature is indicated)



corner of the room. Due to the strong statistical bias towards an even distribution of energy, momenta and position, such an occurrence has incredibly low probability, but it is nonetheless possible, a fact which caused great discomfort with the scientific community at the time.

It is often convenient to work in terms of the occupancy of *energy levels* rather than *states* (phase space cells). To relate the Boltzmann result to energy levels, we must take into account the number of states in a given energy level, termed the *degeneracy* and denoted g_j (we reserve i as the labelling of states). The occupation of the j th energy level is then,

$$N_j = g_j f_B(E_j). \quad (2.5)$$

2.4 Quantum Particles

Having introduced classical particles, their statistics and the equilibrium properties of the ideal gas, now we turn to the quantum case. The statistics of quantum particles, developed in the 1920s, was pivotal to the development of quantum mechanics, pre-dating the well-known Schrödinger equation and uncertainty principle.

2.4.1 A Chance Discovery

Quantum physics arose from the failure of classical physics to describe the emission of radiation from a black body in the ultraviolet range (the “ultraviolet catastrophe”). In 1900, Max Planck discovered a formula which empirically fit the data for all wavelengths and led him to propose that energy is emitted in discrete quanta of units hf (h being Planck’s constant and f the radiation frequency). Einstein extended this idea with his 1905 prediction that the light itself was quantized.

The notion of quantum particles was discovered by accident. Around 1920, the Indian physicist Satyendra Bose was giving a lecture on the failure of the classical

theory of light using statistical arguments; a subtle mistake led to him prove the opposite. Indeed, he was able to derive Planck’s empirical formula from first principles, based on the assumptions that (a) the radiation particles are indistinguishable and (b) phase space was discretized into cells of size h^3 . Bose struggled at first to get these results published and sought support from Nobel Laureate Einstein; Bose’s paper “Planck’s law and the light quantum hypothesis” was then published in 1924 [3]. Soon after Einstein extended the idea to particles with mass in the paper “Quantum theory of the monoatomic ideal gas” [4].

The division of phase space was mysterious. Bose wrote “Concerning the kind of subdivision of this type, nothing definitive can be said”, while Einstein confided in a colleague that Bose’s “derivation is elegant but the essence remains obscure”. It is now established as a fundamental property of particles, consistent with de Broglie’s notion of wave-particle duality (that particles are smeared out, over a lengthscale given by the de Broglie wavelength $\lambda_{\text{dB}} = h/p$) and with Heisenberg’s uncertainty principle (that the position and momentum of a particle have an inherent uncertainty $\Delta x \Delta y \Delta z \Delta p_x \Delta p_y \Delta p_z = h^3$). Each cell represents a distinct quantum state. The indistinguishability of particles follows since it becomes impossible to distinguish two blurry particles in close proximity in phase space.

2.4.2 Bosons and Fermions

Quantum particles come in two varieties—*bosons* and *fermions*:

Fermions Soon after Bose and Einstein’s work, Fermi and Dirac developed *Fermi-Dirac statistics* for fermions. Fermions possess half-integer spin, and include electrons, protons and neutrons. Fermions obey the Pauli exclusion principle (Pauli, 1925), which states that two identical fermions cannot occupy the same quantum state simultaneously.

Bosons Bosons obey Bose–Einstein statistics, as developed by Bose and Einstein (above), and include photons and the Higgs boson. Bosons have integer spin, and since spin is additive, composite bosons may be formed from equal numbers of fermions, e.g. ^4He , ^{87}Rb and ^{23}Na . Unlike fermions, any number of bosons can occupy the same quantum state simultaneously.

The indistinguishability of quantum particles, and the different occupancy rules for bosons and fermions, affect their statistical behaviour. Consider 2 quantum particles across 3 cells, as shown in Fig. 2.5. Since the particles are indistinguishable, we can no longer label them. For bosons there are six microstates; for fermions there are only three (compared to nine for classical particles, Fig. 2.2). The relative probability of paired states to unpaired states is $\frac{1}{3}$, $\frac{1}{2}$ and 0 for classical particles, bosons and fermions, respectively. Bosons are the most gregarious, having the greatest tendency to bunch up, while fermions are the most anti-social of all and completely avoid each other.

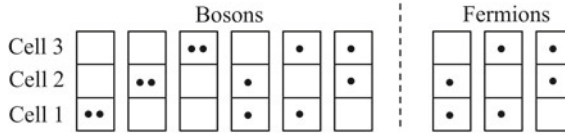


Fig. 2.5 Possible configurations of two bosons (*left*) and two fermions (*right*) across three equally-accessible cells. The classical case was shown in Fig. 2.2

2.4.3 The Bose–Einstein and Fermi–Dirac Distributions

Boltzmann’s mathematical trick of discretizing classical phase space becomes physical reality in the quantum world, and the same methodology can be applied to find the distribution functions for bosons and fermions (accounting for their indistinguishability and occupancy rules). The Bose–Einstein and Fermi–Dirac particle distribution functions, which describe the mean distribution of bosons and fermions over energy E in an ideal gas, are,

$$f_{\text{BE}}(E) = \frac{1}{e^{(E-\mu)/k_{\text{B}}T} - 1}, \quad (2.6)$$

$$f_{\text{FD}}(E) = \frac{1}{e^{(E-\mu)/k_{\text{B}}T} + 1}. \quad (2.7)$$

The rather insignificant looking $-1/+1$ terms in the denominators have profound consequences. Figure 2.6 compares the Boltzmann, Bose–Einstein and Fermi–Dirac distributions.

We make the following observations of the distributions functions:

- To be physical, the distribution functions must satisfy $f \geq 0$ (for all E). This implies that $\mu \leq 0$ for the Bose–Einstein distribution. For the Fermi–Dirac and Boltzmann distributions, μ can take any value and sign.

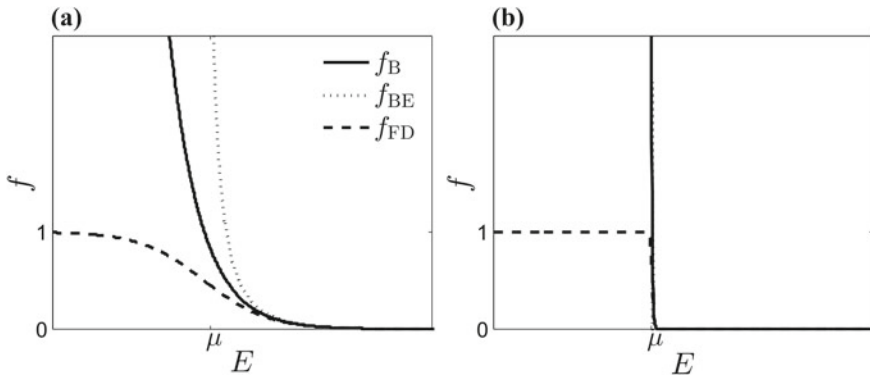


Fig. 2.6 The Boltzmann, Bose–Einstein and Fermi–Dirac distribution functions for **a** $T \gg 0$ and **b** $T \approx 0$

- For $(E - \mu)/k_B T \gg 1$, the Bose–Einstein and Fermi–Dirac distributions approach the Boltzmann distribution. Here, the average state occupancy is much less than unity, such that the effects of particle indistinguishability become negligible. Note that the classical limit condition $(E - \mu)/k_B T \gg 1$ should not be interpreted too directly, as it seems to predict, counter-intuitively, that low temperatures favour classical behaviour; this is because μ itself has a non-trivial temperature dependence.
- As $E \rightarrow \mu$ from above, the Bose–Einstein distribution diverges, i.e. particles accumulate in the lowest energy states.
- For $E \ll \mu$, the Fermi–Dirac distribution saturates to one particle per state, as required by the Pauli exclusion principle.
- For decreasing temperature, the distributions develop a sharper transition about $E = \mu$, approaching step-like forms for $T \rightarrow 0$.

2.5 The Ideal Bose Gas

A year after Einstein and Bose set forth their new particle statistics for a gas of bosons, Einstein published “Quantum theory of the monoatomic ideal gas: a second treatise” [5], elaborating on this topic. Here he predicted Bose–Einstein condensation. We now follow Einstein’s derivation of this phenomena and predict some key properties of the gas.

2.5.1 Continuum Approximation and Density of States

We consider an ideal (non-interacting) gas of bosons confined to a box, with energy level occupation according to the Bose–Einstein distribution (2.6). For mathematical convenience we approximate the discrete energy levels by a continuum, valid providing there are a large number of accessible energy levels. Replacing the level variables with continuous quantities ($E_j \mapsto E$, $g_j \mapsto g(E)$ and $N_j \mapsto N(E)$), the number of particles at energy E is written,

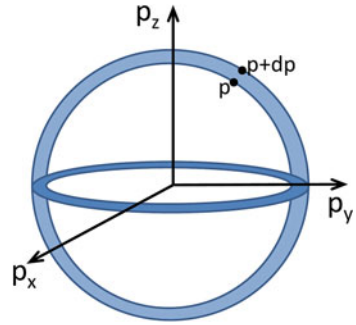
$$N(E) = f_{\text{BE}}(E) g(E) = \frac{g(E)}{e^{(E-\mu)/k_B T} - 1}, \quad (2.8)$$

where $g(E)$ is the *density of states*. The total number of particles and total energy follow as the integrals,

$$N = \int N(E) \, dE, \quad (2.9)$$

$$U = \int E N(E) \, dE. \quad (2.10)$$

Fig. 2.7 The volume of momentum space from p to $p + dp$ is a spherical shell in 3D momentum space



These are integrated in energy upwards from the $E = 0$ ($j = 1$) ground state.

The density of states $g(E)$ is defined such that the total number of possible states in phase space \mathcal{N}_{ps} is,

$$\mathcal{N}_{\text{ps}} = \int g(E) dE = \int g(p) dp, \quad (2.11)$$

where we have also provided the corresponding expression in terms of momentum p , which is more convenient to work with. The quantity $g(p)dp$ represents the number of states lying between momenta p and $p + dp$. These states occupy a (6D) volume in phase space which is the product of their (3D) volume in position space and their (3D) volume in momentum space. The former is the box volume, \mathcal{V} . For the latter, the range p to $p + dp$ represents a spherical shell in momentum space of inner radius p and thickness dp , as illustrated in Fig. 2.7, with momentum-space volume $4\pi p^2 dp$. Hence the phase space volume is $4\pi p^2 \mathcal{V} dp$. Now recall that each quantum state takes up a volume h^3 in phase space. Thus the number of states between p and $p + dp$ is,

$$g(p)dp = \frac{4\pi p^2 \mathcal{V}}{h^3} dp. \quad (2.12)$$

Using the momentum-energy relation $p^2 = 2mE$, its differential form $dp = \sqrt{m/2E} dE$, and the relation $g(E) dE = g(p) dp$, Eq. (2.12) leads to,

$$g(E) = \frac{2\pi(2m)^{\frac{3}{2}} \mathcal{V}}{h^3} E^{\frac{1}{2}}. \quad (2.13)$$

This is the density of states for an ideal gas confined to a box of volume \mathcal{V} . There are a diminishing amount of states in the limit of zero energy, and an increasing amount with larger energy.

While the *occupancy of a state* goes like $1/(e^{(E-\mu)/k_B T} - 1)$ and diverges as $E \rightarrow \mu$, the *occupancy of an energy level* goes like $E^{\frac{1}{2}}/(e^{(E-\mu)/k_B T} - 1)$ and diminishes as $E \rightarrow 0$ (due to the decreasing amount of available states in this limit). These two distributions are compared in Fig. 2.8a.

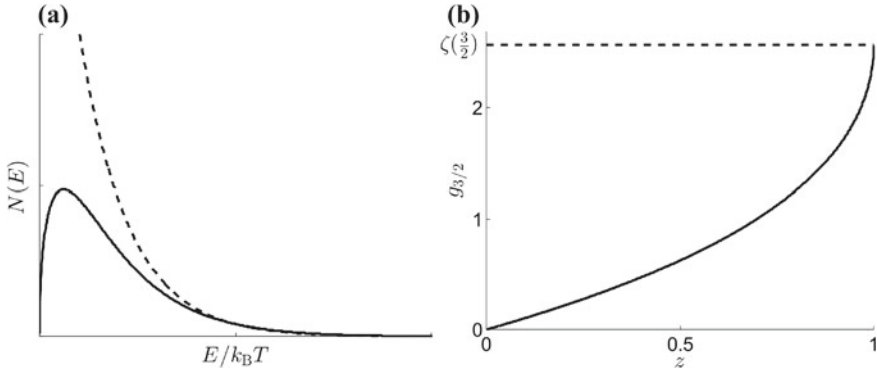


Fig. 2.8 **a** The occupancy of energy levels $N(E)$ (solid line), compared to the Bose–Einstein distribution f_{BE} (dashed line). The former vanishes as $E \rightarrow 0$ due to the diminishing density of states in this limit. **b** The function $g_{\frac{3}{2}}(z) = \sum_{p=1}^{\infty} z^p / p^{\frac{3}{2}}$ over the relevant range $0 < z \leq 1$

2.5.2 Integrating the Bose–Einstein Distribution

Using Eqs. (2.8, 2.13) we can write the number of particles (2.9) as,

$$N = \frac{2\pi(2m)^{\frac{3}{2}} \mathcal{V}}{h^3} \int_0^{\infty} \frac{E^{\frac{1}{2}}}{e^{(E-\mu)/k_{\text{B}}T} - 1} dE. \quad (2.14)$$

We seek to evaluate this integral. To assist us, we quote the general integral,²

$$\int_0^{\infty} \frac{x^{\alpha}}{e^x/z - 1} dx = \Gamma(\alpha + 1) g_{\alpha+1}(z), \quad (2.15)$$

where $\Gamma(x) = \int_0^{\infty} t^{x-1} e^{-t} dt$ is the *Gamma function*.³ We have also defined a new function, $g_{\beta}(z) = \sum_{p=1}^{\infty} \frac{z^p}{p^{\beta}}$; an important case is when $z = 1$ for which it reduces to the *Riemann zeta function*,⁴ $\zeta(\beta) = \sum_{p=1}^{\infty} \frac{1}{p^{\beta}}$.

²This result can be derived by introducing new variables $z = e^{\mu/k_{\text{B}}T}$ and $x = E/k_{\text{B}}T$ to rewrite part of integrand in the form $ze^{-x}/(1 - ze^{-x})$, and then writing as a power series expansion.

³Relevant values for us are $\Gamma(3/2) = \sqrt{\pi}/2$ and $\Gamma(5/2) = 3\sqrt{\pi}/4$.

⁴Relevant values for us are $\zeta(3/2) = 2.612$ and $\zeta(5/2) = 1.341$.

Taking $\alpha = \frac{1}{2}$, $x = E/k_B T$ and $z = e^{\mu/k_B T}$ in the general result (2.15), we evaluate Eq. (2.14) as,

$$N = \frac{(2\pi m k_B T)^{\frac{3}{2}} \mathcal{V}}{h^3} g_{\frac{3}{2}}(z), \quad (2.16)$$

where we have used the result $\Gamma(3/2) = \sqrt{\pi}/2$. Note that the relevant range of z is $0 < z \leq 1$: the lower limit is required since $z = e^{\mu/k_B T} > 0$ while the upper limit $z \leq 1$ is required to prevent negative populations. Note also that $\mu \leq 0$ over this range, as required for the Bose–Einstein distribution (recall Sect. 2.4.3). In Fig. 2.8b we plot $g_{\frac{3}{2}}(z)$ over this range.

2.5.3 Bose–Einstein Condensation

The prediction of Bose–Einstein condensation in the style of Einstein arises directly from Eq. (2.16). Consider adding particles to the box, while at constant temperature. An increase in N is accommodated by an increase in the function $g_{\frac{3}{2}}(z)$. However, $g_{\frac{3}{2}}(z)$ is finite, reaching a maximum value of $g_{\frac{3}{2}} = \zeta(\frac{3}{2}) = 2.612$ at $z = 1$. In other words, the system becomes *saturated* with particles. This critical number of particles, denoted N_c , follows as,

$$N_c = \frac{(2\pi m k_B T)^{\frac{3}{2}} \mathcal{V}}{h^3} \zeta(\frac{3}{2}). \quad (2.17)$$

Our derivation predicts a limit to how many particles the Bose–Einstein distribution can hold, but common sense tells us that it should always be possible to add more particles to the box. In fact, we made a subtle mistake. In calculating N we replaced the summation over discrete energy levels (from the $i = 1$ ground state upwards) by an integral over a continuum of energies (from $E = 0$ upwards). However, this continuum approximation does not properly account for the population of the ground state, since the density of states, $g(E) \propto E^{\frac{1}{2}}$, incorrectly predicts zero population in the ground state. What we have predicted is the *saturation of the excited states*; any additional particles added to the system enter the ground state (which comes at no energetic cost). For $N \gg N_c$, the ground state acquires an anomalously large population.

As Einstein put it [5], “a number of atoms which always grows with total density makes a transition to the ground quantum state, whereas the remaining atoms distribute themselves... A separation occurs; a part condenses, the rest remains a saturated ideal gas.” This effect is *Bose–Einstein condensation*, and the collection of particles in the ground state is the *Bose–Einstein condensate*. The effect is a condensation in momentum space, referring to the occupation of the zero momentum state. In practice, when the system is confined by a potential, a condensation in real space also takes place, towards the region of lowest potential. Bose–Einstein condensation is a *phase transition*, but whereas conventional phase transitions (e.g. transformation

from gas to liquid or liquid to solid) are driven by particle interactions, Bose–Einstein condensation is driven by the particle statistics.

Based on the above hindsight, we note that the total atom number N appearing in Eqs. (2.9), (2.14) and (2.16) should be replaced by the number in excited states, N_{ex} .

2.5.4 Critical Temperature for Condensation

If, instead, the particle number and volume are fixed, then there exists a critical temperature T_c below which condensation occurs. The population of excited particles at a given temperature is given by Eq. (2.16). For $T > T_c$, this is sufficient to accommodate all of the particles, and the gas is in the normal phase. As temperature is lowered, however, the excited state capacity also decreases. At the point where the excited states no longer accommodate all the particles, Bose–Einstein condensation occurs. The critical temperature is obtained by setting $z = 1$ in Eq. (2.16) and rearranging for T ,

$$T_c = \frac{h^2}{2\pi m k_B} \left(\frac{N}{\zeta(\frac{3}{2})V} \right)^{\frac{2}{3}}. \quad (2.18)$$

For further decreases in temperature, N_{ex} decreases and so more and more particles must enter the ground state. In the limit $T \rightarrow 0$, excited states can carry no particles and all particles enter the condensate.

2.5.5 Condensate Fraction

A useful quantity for characterising the gas is the *condensate fraction*, that is, the proportion of particles which reside in the condensate, N_0/N . Let us consider its variation with temperature. Writing $N = N_0 + N_{\text{ex}}$ leads to,

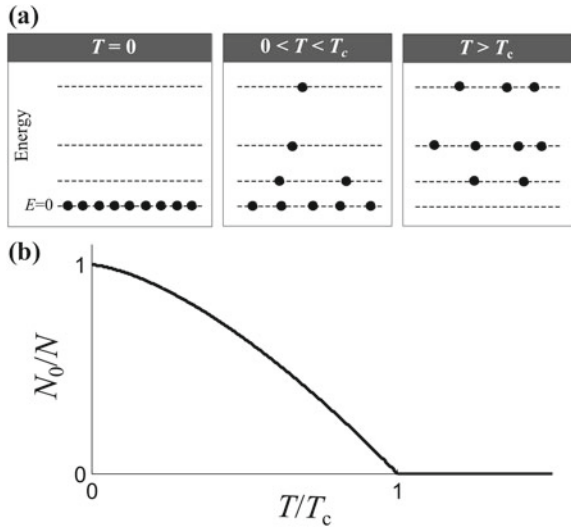
$$\frac{N_0}{N} = 1 - \frac{N_{\text{ex}}}{N}. \quad (2.19)$$

For $T \leq T_c$, the excited population N_{ex} is given by Eq. (2.16) with $z = 1$, and the total population is given by Eq. (2.14) with $z = 1$ and $T = T_c$. Substituting both into the above gives,

$$\frac{N_0}{N} = 1 - \left(\frac{T}{T_c} \right)^{3/2}. \quad (2.20)$$

For $T > T_c$, we expect $N_0/N \approx 0$. This behaviour is shown in Fig. 2.9.

Fig. 2.9 **a** Illustration of energy level occupations in the boxed ideal Bose gas. At $T = 0$ all particles lie in the ground state. For $0 < T < T_c$, some particles are in excited levels but there is still macroscopic occupation of the ground state. For $T > T_c$, there is negligible occupation of the ground state. **b** Variation of condensate fraction, N_0/N , with temperature, as per Eq. (2.20)



2.5.6 Particle-Wave Overlap

Bose–Einstein condensation occurs when $N > N_c$, with N_c given by Eq. (2.17). It is equivalent to write this criterion in terms of the number density of particles, $n = N/V$, as,

$$n > \zeta\left(\frac{3}{2}\right) \frac{(2\pi mk_B T)^{3/2}}{h^3}. \quad (2.21)$$

According to de Broglie, particles behave like waves, with a wavelength $\lambda_{dB} = h/p$. For a thermally-excited gas, the particle wavelength is $\lambda_{dB} = \frac{h}{\sqrt{2\pi mk_B T}}$. Employing this, the above criterion becomes,

$$n\lambda_{dB}^3 > \zeta\left(\frac{3}{2}\right). \quad (2.22)$$

Upon noting that the average inter-particle distance $d = n^{-1/3}$ and $\zeta(\frac{3}{2})^{1/3} \sim 1$ we arrive at,

$$\lambda_{dB} \gtrsim d. \quad (2.23)$$

Thus, Bose–Einstein condensation coincides with the condition that the particle waves overlap with each other, as depicted in Fig. 2.10. The individual particles become smeared out into one giant wave of matter, the condensate.

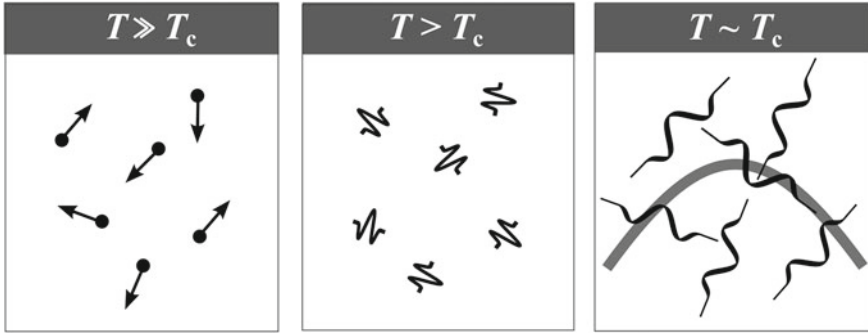


Fig. 2.10 Schematic of the transition between a classical gas and a Bose–Einstein condensate. At high temperatures ($T \gg T_c$) the gas is a thermal gas of point-like particles. At low temperatures (but still exceeding T_c) the de Broglie wavelength λ_{dB} becomes significant, yet smaller than the average spacing d . At T_c , the matter waves overlap ($\lambda_{dB} \sim d$), marking the onset of Bose–Einstein condensation

2.5.7 Internal Energy

The internal energy of the gas U is determined by the excited states only, since the ground state possesses zero energy; therefore we can express U by integrating across the excited state particles as,

$$U = \int_0^{\infty} E N_{\text{ex}}(E) dE. \quad (2.24)$$

Upon evaluating this integral below and above T_c we find,

$$U = \begin{cases} \frac{3}{2} \frac{\zeta(5/2)}{\zeta(3/2)} N k_B T \left(\frac{T}{T_c} \right)^{3/2} & \text{for } T < T_c, \\ \frac{3}{2} N k_B T & \text{for } T \gg T_c. \end{cases} \quad (2.25)$$

The $T \gg T_c$ result is consistent with the classical equipartition theorem for an ideal gas, which states that each particle has on average $\frac{1}{2} k_B T$ of kinetic energy per direction of motion. The different behavior for $T < T_c$ confirms the presence of a distinct state of matter.

2.5.8 Pressure

The pressure of an ideal gas is $P = 2U/3V$. From Eq. (2.25), then for $T \gg T_c$ we recover the standard result for a classical ideal gas that $P \propto T/V$. For $T < T_c$, and recalling that $T_c \propto 1/V^{2/3}$, we find that $P \propto T^{5/2}$. The pressure of the condensate is zero at absolute zero and does not depend on the volume of the box! A consequence of this is that the condensate has infinite compressibility, as explored in Problem 2.6.

2.5.9 Heat Capacity

The heat capacity of a substance is the energy required to raise its temperature by unit amount. At constant volume it is defined as,

$$C_V = \left(\frac{\partial U}{\partial T} \right)_V. \quad (2.26)$$

From Eq. (2.25) we find,

$$C_V = \begin{cases} 1.93 N k_B T^{3/2} & \text{for } T < T_c, \\ \frac{3}{2} N k_B & \text{for } T \gg T_c. \end{cases} \quad (2.27)$$

A more precise treatment, describing the dependence at intermediate temperatures, can be found in Ref. [6]. The form of $C_V(T)$ is depicted in Fig. 2.11, showing a cusp-like dependence around T_c . In general, discontinuities in the gradient of $C_V(T)$ are signatures of phase transitions between distinct states of matter. The similarity of

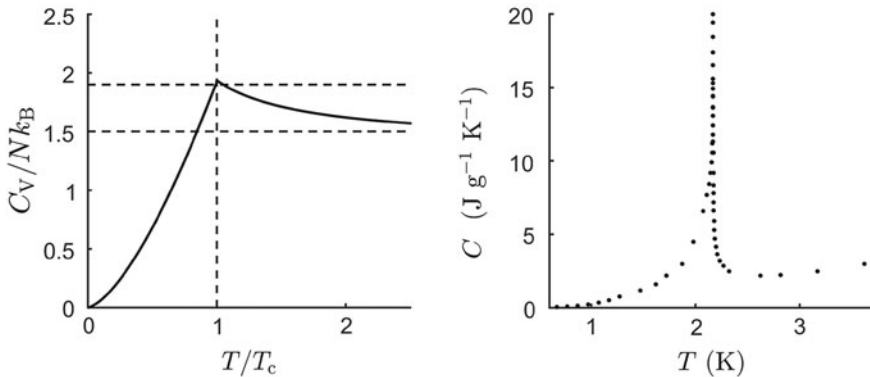


Fig. 2.11 *Left* Heat capacity C_V of the ideal Bose gas as a function of temperature T . *Right* Experimental heat capacity data of liquid Helium, taken from [7], about the λ -point of 2.2 K. Both curves show a similar cusped structure

this prediction to measured heat capacity curves for Helium about the λ -point was key evidence in linking helium II to Bose–Einstein condensation.

2.5.10 Ideal Bose Gas in a Harmonic Trap

2.5.10.1 Critical Temperature and Condensate Fraction

In typical experiments, atomic Bose–Einstein condensates are confined by harmonic (quadratic) potentials, rather than boxes,⁵ with the general form,

$$V(x, y, z) = \frac{1}{2}m (\omega_x^2 x^2 + \omega_y^2 y^2 + \omega_z^2 z^2), \quad (2.28)$$

where m is the atomic mass, and ω_x, ω_y and ω_z are trap frequencies which characterise the strength of the trap in each direction. Here the density of states is modified, being $g(E) = E^2/(2\hbar^3\omega_x\omega_y\omega_z)$ in 3D. This leads, for example, to a critical temperature of the form,

$$T_c = \frac{\hbar}{k_B} (\omega_x\omega_y\omega_z)^{1/3} \left[\frac{N}{\zeta(3)} \right]^{1/3}, \quad (2.29)$$

and for the condensate fraction to vary with temperature as,

$$\frac{N_0}{N} = 1 - \left(\frac{T}{T_c} \right)^3. \quad (2.30)$$

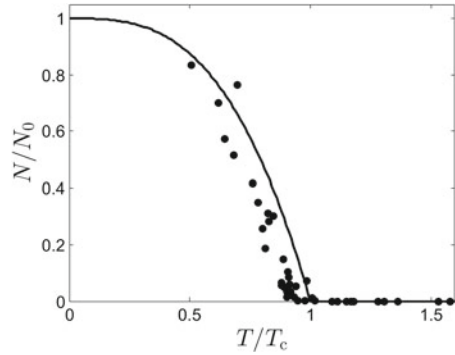
These predictions agree well with experimental measurements of harmonically-trapped atomic BECs, as seen in Fig. 2.12. This is despite the fact that atomic BECs are not *ideal* but feature significant interactions between atoms.

2.5.10.2 Density Profile

We can deduce the density profile of the (non-interacting) condensate in a harmonic trap as follows. The ground quantum state in a harmonic trap is the ground harmonic oscillator state. For simplicity, assume a spherically-symmetric trap with $\omega_x = \omega_y = \omega_z \equiv \omega_r$. The ground quantum state for a single particle is provided by solving the time-independent Schrödinger equation under this harmonic potential, giving the ground harmonic oscillator wavefunction $\psi(r) = \left(\frac{m\omega}{\pi\hbar}\right)^{3/4} e^{-m\omega r^2/2\hbar}$. The quantity $|\psi(r)|^2$ represents the probability of finding the particle at position r . For a condensate of N_0 such particles, with $N_0 \gg 1$, the particle density profile will follow as,

⁵Box-like traps [8, 9] are also possible, and allow the condensate to have uniform density, facilitating comparison with the theory of homogeneous condensates.

Fig. 2.12 Variation of condensate fraction N_0/N with temperature for a harmonically-trapped BEC, with the ideal-gas predictions (solid line) compared to experimental measurements from Ref. [10] (circles), with $T_c = 280$ nK



$$n(r) = N_0 |\psi|^2 = N_0 (\hbar \ell_r^2)^{-3/2} e^{-r^2/\ell_r^2}, \quad (2.31)$$

where we have introduced the harmonic oscillator length $\ell_r = \hbar/m\omega_r$ which characterises the width of the density distribution.

We can also deduce the density profile of the thermal gas. Taking the classical limit, the atoms will be distributed over energy according to the Boltzmann distribution $N(E) \propto e^{-E/k_B T}$. The trapping potential $V(r)$ allows us to map energy (potential) to position, leading to a spatial particle distribution,

$$n(r) = N_{\text{ex}} (\hbar \ell_{r,\text{th}}^2)^{-3/2} e^{-r^2/\ell_{r,\text{th}}^2}, \quad (2.32)$$

where $\ell_{r,\text{th}} = \sqrt{2k_B T/m\omega_r^2}$ characterises the width of the thermal gas and the profile has been normalized to N_{ex} atoms. For increased temperature, the atoms have higher average energy and climb further up the trap walls, leading to a wider profile. While the profiles of the ideal condensate and ideal thermal gas are both Gaussian in space, their widths have different functional forms. In particular, the width of the thermal gas depends on temperature, whereas the condensate width does not.

The typical experimental protocol to form a BEC proceeds by cooling a relatively warm gas towards absolute zero. Above T_c the gas has a broad thermal distribution, which shrinks during cooling. As T_c is under-passed, the condensate distribution forms. In typical atomic BEC experiments, $\ell_r \ll \ell_{r,\text{th}}$, such that this is distinctly narrower than the thermal gas, and the combined density profile is bimodal. Under further cooling, the condensate profile grows (with fixed width) at the expense of the thermal profile, and for $T \ll T_c$ the thermal gas is negligible. In reality, atomic interactions modify the precise shapes of the density profiles but this picture *qualitatively* describes what is observed in experiments (see Figs. 1.3 and 1.4).

2.6 Ideal Fermi Gas

We outline the corresponding behaviour of the ideal Fermi gas. Since (identical) fermions are restricted to up to one per state, Bose–Einstein condensation is prohibited, and the Fermi gas behaves very differently as $T \rightarrow 0$. At $T = 0$ the Fermi–Dirac distribution (2.7) reduces to a step function,

$$f_{\text{FD}}(E) = \begin{cases} 1 & \text{for } E \leq E_{\text{F}}, \\ 0 & \text{for } E > E_{\text{F}}. \end{cases} \quad (2.33)$$

All states are occupied up to an energy threshold E_{F} , termed the *Fermi energy* (equal to the $T = 0$ chemical potential). With this simplified distribution it is straightforward to integrate the number of particles,

$$N = \int_0^{E_{\text{F}}} N(E) \, dE = \int_0^{E_{\text{F}}} g(E) f_{\text{FD}}(E) \, dE = \frac{4\pi\mathcal{V}}{3} \left(\frac{2mE_{\text{F}}}{h^2} \right)^{3/2}, \quad (2.34)$$

where we have used the density of states (2.13). Note that the continuum approximation $N = \int g(E) N(E) \, dE$ holds for $N \gg 1$ fermions since the unit occupation of the ground state is always negligible. Rearranging for the Fermi energy in terms of the particle density $n = N/\mathcal{V}$ gives,

$$E_{\text{F}} = \frac{\hbar^2}{2m} (6\pi^2 n)^{2/3}. \quad (2.35)$$

From this we define the Fermi momentum $p_{\text{F}} = \hbar k_{\text{F}}$ where $k_{\text{F}} = (6\pi^2 n)^{1/3}$ is the Fermi wavenumber. In momentum space, all states are occupied up to momentum p_{F} , termed the *Fermi sphere*.

Similarly, the total energy of the gas at $T = 0$ is,

$$U = \int N(E) E \, dE = \frac{4\pi\mathcal{V}}{5} \left(\frac{2m}{h^2} \right)^{3/2} E_{\text{F}}^{5/2} = \frac{3}{5} N E_{\text{F}}. \quad (2.36)$$

From the pressure relation for an ideal gas, $P = 2U/3\mathcal{V}$, the pressure of the ideal Fermi gas at $T = 0$ is,

$$P = \frac{2}{5} n E_{\text{F}}. \quad (2.37)$$

This pressure is finite even at $T = 0$, unlike the Bose and classical gases, and does not arise from thermal agitation. Instead it is due to the stacking up of particles in energy levels, as constrained by the quantum rules for fermions. This *degeneracy pressure* prevents very dense stars, such as neutron stars, from collapsing under their own gravitational fields.

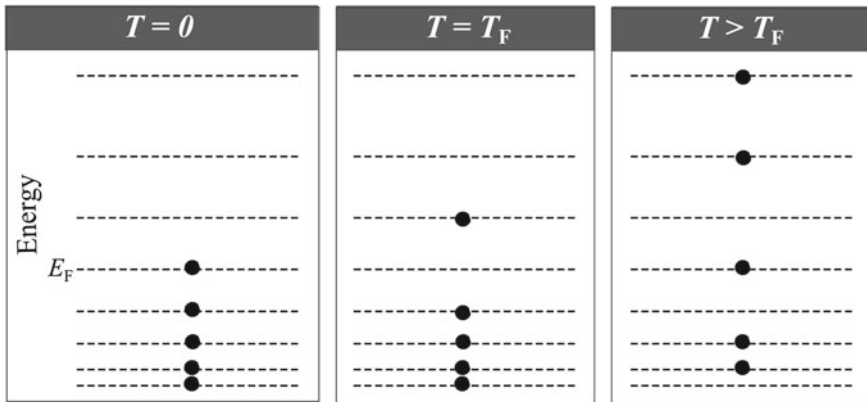


Fig. 2.13 Energy level occupations for an ideal Fermi gas. At $T = 0$, there is unit occupation of states up to the Fermi energy. At $T = T_F$, there is some excitation of states around $E = E_F$. For $T \gg T_F$, the system approaches the classical limit, with particles occupying many high-energy states

As temperature is increased from zero, the step-like Fermi-Dirac distribution becomes broadened about $E = E_F$, representing that some high energy particles become excited to energies exceeding E_F . It is useful to define the *Fermi temperature* $T_F = E_F/k_B$. At low temperatures $T \sim T_F$, only particles in states close to E_F can be excited out of the Fermi sphere, and the system is still dominated by the stacking of particles. For high temperatures $T \gg T_F$, there is significant excitation of most particles, thermal effects dominates, and the system approaches the classical Boltzmann result. The Fermi temperature is associated with the onset of degeneracy, i.e. when quantum effects dominate the system. These regimes are depicted in Fig. 2.13.

Now consider the Fermi gas to be confined in a harmonic trap. For $T \gg T_F$ the gas will have a broad, classical profile. As T is decreased, the profile will narrow but eventually saturates below T_F due to degeneracy pressure. The width of the Fermi gas at zero temperature is proportional to $N^{1/6}\ell_r$ [11], such that, for $N \gg 1$, this cloud is much wider than its classical and Bose counterparts. This picture is confirmed by the experimental images in Fig. 1.4.

2.7 Summary

In his 1925 prediction of Bose–Einstein condensation of an ideal gas, Einstein suggested hydrogen, helium and the electron gas were the best candidates for observing Bose–Einstein condensation. However, the former candidates are no longer gases at the required densities, and the latter (as soon realized) is fermionic. For over a decade, Bose–Einstein condensation had “the reputation of having only a purely

imaginary character” [12], deemed too fragile to occur in real gases with their finite size and particle interactions. In 1938 Einstein’s idea became revived when Fritz London recognized the similarity to the heat capacity curves in Helium as it entered the superfluid phase. It took several more decades to cement this link with microscopic theory. Bose–Einstein condensation is now known to underlie superfluid He^4 and He^3 , superconductors and the ultracold atomic Bose gases. We explore the latter in the next chapter.

Problems

2.1 Consider a system with 6 classical particles, total energy of 6ϵ , and 7 cells with energies $0, \epsilon, 2\epsilon, 3\epsilon, 4\epsilon, 5\epsilon$ and 6ϵ . Complete the table below by entering the cell populations for each macrostate, the statistical weighting for each macrostate W , and the average population per cell $\bar{N}(E)$ (averaged over macrostates). What is the most probable macrostate? Plot $\bar{N}(E)$ versus E . It should be evident that the average distribution approximates the Boltzmann distribution, despite the small number of particles.

Cell energy E	Macrostates		
	1	...	11
6ϵ	?	...	?
5ϵ	?	...	?
\vdots	\vdots	...	\vdots
ϵ	?	...	?
0	?	...	?
Statistical weighting W	?	...	?

2.2 Consider a system with N classical particles distributed over 3 cells (labelled 1, 2, and 3) of energy $0, \epsilon$ and 2ϵ . The total energy is $E = 0.5N\epsilon$.

- Obtain an expression for the number of microstates in terms of N and N_3 , the population of cell 3.
- Plot the number of microstates as a function of N_2 (which parameterises the macrostate) for $N = 50$. Repeat for $N = 100$ and 500 . Note how the distribution changes with N . What form do you expect the distribution to tend towards as N is increased to much larger values?

2.3 Consider an ideal gas of bosons in two dimensions, confined within a two-dimensional box of volume \mathcal{V}_{2D} .

- Derive the density of states $g(E)$ for this two-dimensional system.
- Using this result show that the number of particles can be expressed as,

$$N_{\text{ex}} = \frac{2\pi m \mathcal{V}_{2D} k_B T}{h^2} \int_0^\infty \frac{z e^{-x}}{1 - z e^{-x}} dx,$$

where $z = e^{\mu/k_B T}$ and $x = E/k_B T$. Solve this integral using the substitution $y = z e^{-x}$.

- (c) Obtain an expression for the chemical potential μ and thereby show that Bose–Einstein condensation is possible only at $T = 0$.

2.4 Equation (2.25) summarizes how the internal energy of the boxed 3D ideal Bose gas scales with temperature. Derive the full expressions for the internal energy for the two regimes (a) $T < T_c$ (for which $z = 1$), and (b) $T \gg T_c$ (for which $z \ll 1$). Extend your results to derive the expressions for the heat capacity given in Eq. (2.27).

2.5 Bose–Einstein condensates are typically confined in harmonic trapping potentials, as given by Eq. (2.28). Using the corresponding density of states provided in Sect. 2.5.10.1:

- Derive the expression for the critical number of particles.
- Derive the expression (2.29) for the critical temperature.
- Determine the expression (2.30) for the variation of condensate fraction N_0/N with T/T_c .
- In one of the first BEC experiments, a gas of 40, 000 Rubidium-87 atoms (atomic mass 1.45×10^{-25} kg) underwent Bose–Einstein condensation at a temperature of 280 nK. The harmonic trap was spherically-symmetric with $\omega_r = 1130$ Hz. Calculate the critical temperature according to the ideal Bose gas prediction. How does this compare to the result for the boxed gas (you may assume the atomic density as $2.5 \times 10^{18} \text{ m}^{-3}$).

2.6 The compressibility β of a gas, a measure of how much it shrinks in response to a compressional force, is defined as,

$$\beta = -\frac{1}{\mathcal{V}} \frac{\partial \mathcal{V}}{\partial P}.$$

Determine the compressibility of the ideal gas for $T < T_c$.

Hint: Since T_c is a function of \mathcal{V} , you should ensure the full \mathcal{V} -dependence is present before differentiating.

References

1. F. Mandl, *Statistical Physics*, 2nd edn. (Wiley, Chichester, 1988)
2. L.D. Landau, E.M. Lifshitz, *Statistical Physics*, 3rd edn. (Elsevier, Oxford, 1980)
3. S.N. Bose, *Z. Phys.* **26**, 178 (1924)
4. A. Einstein, *Kgl. Preuss. Akad. Wiss.* **261** (1924)
5. A. Einstein, *Kgl. Preuss. Akad. Wiss.* **3** (1925)

6. L.P. Pitaevskii, S. Stringari, *Bose-Einstein Condensation (International Series of Monographs on Physics)* (Oxford Science Publications, Oxford, 2003)
7. M.J. Buckingham, W.M. Fairbank, The nature of the lambda-transition in liquid helium, in *Progress in Low Temperature Physics*, vol. 3, ed. by C.J. Gorter (North Holland, Amsterdam, 1961)
8. A.L. Gaunt, T.F. Schmidutz, I. Gotlibovych, R.P. Smith, Z. Hadzibabic, *Phys. Rev. Lett.* **110**, 200406 (2013)
9. L. Chomaz et al., *Nat. Comm.* **6**, 6162 (2015)
10. J.R. Ensher, D.S. Jin, M.R. Matthews, C.E. Wieman, E.A. Cornell, *Phys. Rev. Lett.* **77**, 4984 (1996)
11. D.A. Butts, D.S. Rokhsar, *Phys. Rev. A* **55**, 4346 (1997)
12. F. London, *Nature* **141**, 643 (1938)

<http://www.springer.com/978-3-319-42474-3>

A Primer on Quantum Fluids

Barenghi, C.F.; Parker, N.G.

2016, XIII, 119 p. 56 illus., 34 illus. in color., Softcover

ISBN: 978-3-319-42474-3